Leuk Lymphoma. 2012 Dec;53(12):2474-8. [doi: 10.3109/10428194.2012.696313]

Chronic myeloid leukemia stem cells display alterations in expression of genes involved in oxidative phosphorylation.

Flis K, Irvine D, Copland M, Bhatia R, Skorski T.

PMID: 22616753

Chronic myeloid leukemia stem cells display alterations in the expression of genes involved in oxidative phosphorylation

Running title: Altered oxidative phosphorylation in CML

Krzysztof Flis[1,2], David Irvine[3], Mhairi Copland[3], Ravi Bhatia[4], Tomasz Skorski[1,*]

[1]Department of Microbiology and Immunology, Temple University, School of Medicine, Philadelphia, PA 19140, USA

[2]Institute of Biochemistry and Biophysics, Polish Academy of Sciences, Warsaw, Poland

[3]Paul O'Gorman Leukemia Research Centre, University of Glasgow, Glasgow, UK.

[4]Division of Hematopoietic Stem Cell and Leukemia Research, Department of Hematology and Hematopoietic Cell Transplantation, City of Hope National Medical Center, Duarte, CA 91010, USA

*Corresponding author: Tomasz Skorski, Department of Microbiology and Immunology, Temple University School of Medicine, 3400 N. Broad Street, MRB 548, Philadelphia, PA 19140, USA, e-mail: tskorski@temple.edu

Key words: CML leukemia stem cells, oxidative phosphorylation, microarray analysis

Abstract

Mitochondrial respiratory chain (MRC) consists of the protein complexes I, II, III, IV, and V to carry oxidative phosphorylation (OXPHOS), which depends on electron transport to generate ATP. Electron “leakage” from MRC generates reactive oxygen species (ROS). Chronic myeloid leukemia in chronic phase (CML-CP) stem cells (LSCs) produce high levels of mitochondrial ROS causing oxidative DNA damage resulting in genomic instability generating imatinib-resistant BCR-ABL1 kinase mutants and additional chromosomal aberrations. Using global mRNA microarray analysis combined with Ingenuity pathway analysis we found that LSCs display enhanced expression of genes encoding MRC complexes I, II, IV, and V. However, expression of genes encoding complex III was deregulated. Treatment with imatinib did not correct the aberrant levels of MRC genes. Therefore we postulate that abnormal expression of MRC genes may facilitate electron “leakage” to promote production of ROS and accumulation of genomic instability in LSCs in imatinib-naive and imatinib-treated patients.

Introduction

Chronic myeloid leukemia in chronic phase (CML-CP) is initiated by the oncogenic BCR-ABL1 tyrosine kinase that transforms hematopoietic stem cells (HSCs) to leukemia stem cells (LSCs) [1]. Deregulated growth of LSCs-derived leukemia progenitor cells (LPCs) leads to the manifestation of the disease. ABL1 tyrosine kinase inhibitors (TKIs), such as imatinib, dasatinib and nilotinib may induce favorable therapeutic responses, but LSCs are intrinsically insensitive to TKIs despite inhibition of BCR-ABL1 kinase [2]. CML-CP cells may at some stage acquire additional genetic changes that confer TKI resistance and induce more aggressive CML blast phase (CML-BP) [3].

Genomic instability may result from enhanced oxidative DNA damage caused by reactive oxygen species (ROS) [4]. Superoxide anion ($\bullet O_2^-$), the first produced ROS molecule, is a moderately stable free radical. Superoxide dismutase uses $\bullet O_2^-$ to generate hydrogen peroxide (H_2O_2), which may be then converted to the highly reactive hydroxyl group (•OH). ROS can damage DNA bases to produce oxo-derivatives such as 7,8-dihydro-8-oxo-2'-deoxyguanosine (8-oxoG) and also induce spontaneous DNA double-strand breaks (DSBs). Unfaithful and/or inefficient repair of these oxidative DNA lesions can generate point mutations and chromosomal aberrations.

We reported recently that CML-CP LSCs and early LPCs accumulate high levels of ROS resulting in accumulation of TKI-resistant BCR-ABL1 kinase mutants and additional chromosomal aberrations [5]. This effect was due to Rac2-mediated modification of the mitochondrial membrane potential ($\Delta\Psi_m$) associated with slower electron flow through mitochondrial respiratory chain (MRC) complex III. This phenomenon facilitated electron "leakage" from the complex III and production of superoxide anion. The current study suggests

that an imbalance in the expression of MRC components may contribute to production of ROS in CML-CP LSCs.

Materials and Methods

Isolation of hematopoietic stem and progenitor cell populations from CML patients and normal donors: Fresh leukapheresis or peripheral blood samples were obtained with written informed consent and approval of the Greater Glasgow and Clyde Ethics Committee (Institutional Review Board) from patients with newly diagnosed chronic phase (n=6), accelerated phase (n=4) or myeloid blast crisis (n=2) CML and healthy donors of peripheral blood stem cells (n=3). Samples were enriched for $CD34^+$ cells using CliniMACS (Miltenyi Biotec Ltd) according to the manufacturer's instructions and cryopreserved in 10% (v/v) DMSO in 5% (w/v) Human Albumin Solution (Baxter Healthcare Ltd). After thawing, $CD34^+$ cells were cultured overnight in serum free medium (SFM) consisting of Iscove's Modified Dulbecco's Medium (IMDM, Sigma-Aldrich) containing a serum substitute (bovine serum albumin, insulin, transferrin; all from StemCell Technologies), 0.1μM 2-mercaptoethanol (Sigma-Aldrich), and a high concentration five growth factor cocktail comprising 100ng/mL Flt3-ligand (Flt3L), 100ng/mL stem cell factor (SCF), and 20ng/mL each of interleukin (IL)-3, IL-6 (all from StemCell Technologies) and granulocyte-colony stimulating factor (G-CSF; Chugai Pharma Europe). $CD34^+$ CML and normal cells were simultaneously stained with lineage (Lin) cocktail-FITC, CD90-PE, CD34-PerCP, CD38-PE-Cy7, CD123-APC and CD45RA-Pacific Blue (all from BD Biosciences) at room temperature for 20 minutes. Unbound antibodies were washed off with PBS/2% fetal calf serum (FCS) and the cells were sorted to isolate the different subpopulations (hematopoietic stem cell [HSC] – $lin^-CD34^+CD38^-CD90^+$; multipotent progenitor [MPP] – $lin^-CD34^+CD38^-CD90^-$; common myeloid progenitor [CMP] – $lin^-CD34^+CD38^+CD123^+CD45RA^-$; granulocyte monocyte progenitor [GMP] – $lin^-CD34^+CD38^+CD123^+CD45RA^{lo}$; and megakaryocyte erythroid progenitor [MEP] – $lin^-CD34^+CD38^+CD123^-CD45RA^-$) using FACSAria (BD Biosciences).

RNA preparation from normal and CML samples and microarray analysis: RNA was prepared from sorted subpopulations of cells using the RNeasy kit (Qiagen). RNA processing and microarray analysis was carried out at the Sir Henry Wellcome Functional Genomics Facility (SHWFGF, University of Glasgow). RNA samples were analyzed on the Affymetrix GeneChip Human Gene 1.0 ST arrays using standard Affymetrix protocols. The raw data CEL files were normalized using gcRMA n Partek Genomic Suite software http://www.partek.com/partekgs. One way ANOVA was performed on the imported, normalized and summarized microarray data to find differently expressed genes between all cell subpopulations and disease states. Lists of differentially expressed genes were created using an FDR limit of 0.05 to control for multiple comparisons but no limit on degree of fold change. These lists were uploaded directly into Ingenuity Pathway Analysis (IPA) software (Ingenuity Systems). To determine which functional groupings of genes were differentially expressed we performed gene ontology ANOVA (GO ANOVA). Partek GS utilizes the gene ontology (GO) database to map genes to standardized functional groupings. The ANOVA model was configured to contrast the different sub-populations and disease states in order to determine the significance and average fold change of each GO category across all the comparator groups. These results were visualized using dot plots where the average expression of all genes in that functional group is represented as a single dot. The average expression is plotted on a log2 scale on the y axis, and each subpopulation in each disease state on the x axis.

Analysis of CML-CP samples treated or not with imatinib: CML-CP patient samples, imatinib treatment and microarray analysis were as described before [6]. Briefly, CML $CD34^{+}CD38^{-}$ cells selected with flow cytometry sorting were treated with 1 μM imatinib or cultured without exposure to the drug (control) for 24 hr (n = 3 each). Total RNA from 5000 cells was extracted with the RNeasy kit (Qiagen), amplified and labeled with GeneChip Two-Cycle Target Labeling and Control Reagents (Affymetrix, Santa Clara, CA), and hybridized to

Affymetrix GeneChip Human Genome U133 Plus 2.0 Arrays. Microarray data analyses were performed with R (version 2.9) with genomic analysis packages (version 2.4) from Bioconductor. Expression data were normalized with the robust multiarray average (RMA) algorithm, with background adjustment, quantile normalization, and median polish summarization. Probe sets with low expression levels or low variability across samples were filtered. For genes with multiple probe sets, the gene level expression was set to be the median of the probe sets. Linear regression was used to model the gene expression with the consideration of 2 3 2 factorial design and matched samples. Differentially expressed genes were identified by calculating empirical Bayes moderated t-statistic, and p values were adjusted by FDR with the ‘‘LIMMA’’ package. Gene Set Enrichment Analysis (GSEA) was performed with GSEA software version 2.04 (http://www.broadinstitute.org/gsea/) for detection of enrichment of predetermined gene sets with t-scores from all 13,812 genes [7]. These lists were uploaded directly into IPA software (Ingenuity Systems).

Results

We performed global gene expression studies on normal and CML hematopoietic stem and progenitor cell populations (HSC, MPP, CMP, GMP and MEP) using the Affymetrix GeneChip Human Gene 1.0 ST arrays. One way ANOVA and GO ANOVA were used to identify differentially expressed single genes and functional groupings of genes, respectively, in comparison to normalized data from HSCs obtained from healthy donors. The gene grouping and individual genes associated with OXPHOS (GO-ID: 6119) such as UQCRB, UQCRC1, UQCRH were significantly de-regulated in CML-CP LSCs compared to normal HSCs, but were not abundantly altered between normal and CML-CP in the different progenitor sub-populations (**Figure 1A, B**; **Supplemental Table 1**). As the disease progressed to CML-AP and CML-BP, expression of OXPHOS genes was highly variable and became more often downregulated in LSCs and LPCs.

Differential expression of genes involved in OXPHOS in CML-CP LSCs compared to normal HSCs was further analyzed using Ingenuity Functional Term (IFT): Oxidative phosphorylation (**Figure 2; Supplemental Table 2**) and Mitochondrial Dysfunction (**Figure 3; Supplemental Table 3**). Both approaches detected uniform upregulation of the expression of genes encoding MRC complex I (NADH-coenzyme Q oxidoreductase) such as NDUFA2, NDUFA3, NDUFA9, NDUFA11, NDUFB6, NDUFB9, NDUFB10, NDUFB11, NDUFAB1, NDUFS4, NDUFS7, NDUFS8 and NDUFV3, MRC complex II (succinate-Q oxidoreductase) such as SDHB, MRC complex IV (cytochrome c oxidase) such as COX5A, COX5B, COX6B1, COX7B and COX11, and MRC complex V (ATP synthase) such as ATP5A1, ATP5B, ATP5C1, ATP5D, ATP5G1, ATP5H, ATP5I and ATP5J2. In contrast, expression of genes encoding MRC complex III (Q-cytochrome c oxidoreductase) were in disarray: CYTB and UQCRB were downregulated whereas CYC1, UQCR10, UQCRC1, UQCRC2, UQCRFS1 and UQCRH were upregulated.

Ingenuity Pathway Analysis (IPA), including the genes identified by IFT, highlighted potential deregulation of the MRC genes in CML-CP LSCs (**Figure 4A**). Interestingly, imatinib treatment did not correct their aberrant expression (**Figure 4B; Supplemental Table 4**).

Discussion

Some cancer stem cells (CSCs), for example breast and lung CSCs, maintain low ROS levels due to several factors, including increased expression of free radicals scavengers, lower quantity of mtDNA and higher $\Delta\Psi_m$ [8,9]. In contrast, LSCs from BCR-ABL1 –positive CML-CP and IDH1/2 mutation –positive AML accumulate high levels of ROS [5,10]. We reported that high levels of ROS in CML-CP LSCs induced oxidative DNA damage resulting in genomic instability which may produce imatinib-resistant BCR-ABL1 kinase mutants and additional chromosomal aberrations leading to the disease relapse and/or malignant progression [5,11,12]. Since CML-CP LSCs, in particular the quiescent sub-population, are refractory to TKIs, genomic instability in these cells is especially dangerous [13]. Identification of the mechanisms of genomic instability in CML-CP LSCs may lead to novel therapeutic modalities preventing the disease relapse/malignant progression in patients under TKI treatment.

At least 50% of ROS in CML-CP LSCs is produced by mitochondria [5]. However, the mechanism responsible for this phenomenon has not been described. Here we report that CML-CP display deregulated expression of the MRC components, which may contribute to overproduction of mitochondrial ROS. Numerous MRC genes appear overexpressed in LSCs suggestimg enhanced OXPHOS, which may reflect enhanced proliferation associated with decreased self-renewal and increased differentiation of LSCs in comparison to normal HSCs [14]. Unexpectedly, two members of MRC complex III, UQCRB and CTYB were downregulated. The reason for this effect is not known, but it may result from transcriptional regulation and/or better adaptation to bone marrow niche conditions [15-17]. Overall, elevated or normal expression of the components of MRC complex I and II suggests that OXPHOS reaction and electron flow can be properly initiated, but deregulated expression of the members of MRC complex III may “derail” and/or slow down the flow of electrons causing their “leakage”. This

speculation is supported by our previous report that Rac2-mediated reduction of $\Delta\Psi_m$ combined with inhibition of the electron flow through MRC complex III facilitated electron "leakage" resulting in high levels of ROS in CML-CP [5].

We reported before that imatinib inhibited BCR-ABL1 kinase and ROS in BCR-ABL1 – positive 32Dcl3 cell line [12]. However, despite inhibition of BCR-ABL1 kinase, imatinib did not significantly reduce ROS in LSCs/LPCs in the presence of growth factors, suggesting that other factors play an important role in generation of high levels of ROS in patient cells [5]. Imatinib did not restore proper expression levels of MRC components in CML-CP LSCs implicating their continuous role in generation of ROS (this work) and accumulation of genomic instability even in imatinib-treated patients [3,13]. Retention of Rac2 activity in imatinib-treated CML-CP cells may contribute to this phenomenon. Functional studies are warranted to determine if postulated deregulation of the expression of MRC genes depends on Rac2 activity or other mechanisms.

Overall, our findings are consistent with the hypothesis that mitochondria present in CML-CP LSCs display a unique "metabolic-bioenergetic-oxidative" phenotype in which dysfunctional MRC generates high levels of mitochondrial ROS and low levels of ATP; the latter effect being compensated by enhanced glucose uptake and aerobic glycolysis [18]. CML-CP progression to CML-BP was accompanied with extensive downregulation of the components of MRC complex I and IV suggesting more pronounced defect.

Acknowledgements

This work was supported in part by grants CA123014 and CA134458 to T.Skorski. D. Irvine is a Chief Scientist's Office Clinical Research Fellow; M. Copland is funded by the Scottish Funding Council (SCD/04) and Leukaemia and Lymphoma Research (No. 11017). Procurement of biospecimens was facilitated by the Glasgow Tissue Biorepository. This study was supported by the Glasgow Experimental Cancer Medicine Centre (ECMC), which is funded by Cancer Research UK and by the Chief Scientist's Office (Scotland).

Declaration of Interests

M. Copland has received research funding from Novartis and Bristol-Myers Squibb, is on Advisory Boards for Bristol Myers Squibb and Pfizer and has received honoraria from Bristol-Myers Squibb, Novartis and Pfizer. R. Bhatia has received honorarium from Novartis. The other authors declare no conflicts of interest.

References

1. Melo JV, Barnes DJ. Chronic myeloid leukaemia as a model of disease evolution in human cancer. Nat Rev Cancer. 2007;7:441-53.
2. Corbin AS, Agarwal A, Loriaux M, Cortes J, Deininger MW, Druker BJ. Human chronic myeloid leukemia stem cells are insensitive to imatinib despite inhibition of BCR-ABL activity. J Clin Invest 2011;121:396-409.
3. Perrotti D, Jamieson C, Goldman J, Skorski T. Chronic myeloid leukemia: mechanisms of blastic transformation. J Clin Invest 2010;120:2254-64.
4. Slupphaug G, Kavli B, Krokan HE. The interacting pathways for prevention and repair of oxidative DNA damage. Mutat Res 2003;531:231-51.
5. Nieborowska-Skorska M, Kopinski PK, Ray R, et al. Rac2-MRC-cIII-generated ROS cause genomic instability in chronic myeloid leukemia stem cells and primitive progenitors. Blood 2012;119:4253-63.
6. Zhang B, Strauss AC, Chu S, et al. Effective targeting of quiescent chronic myelogenous leukemia stem cells by histone deacetylase inhibitors in combination with imatinib mesylate. Cancer Cell 2010;17:427-42.
7. Subramanian A, Tamayo P, Mootha VK, et al. Gene set enrichment analysis: a knowledge-based approach for interpreting genome-wide expression profiles. Proc Natl Acad Sci U S A 2005;102:15545-50.
8. Diehn M, Cho RW, Lobo NA, et al. Association of reactive oxygen species levels and radioresistance in cancer stem cells. Nature 2009;458:780-3.
9. Ye XQ, Li Q, Wang GH, et al. Mitochondrial and energy metabolism-related properties as novel indicators of lung cancer stem cells. Int J Cancer 2011;129:820-31.
10. Abdel-Wahab O, Levine RL. Metabolism and the leukemic stem cell. J Exp Med 2010;207:677-80.
11. Koptyra M, Cramer K, Slupianek A, Richardson C, Skorski T. BCR/ABL promotes accumulation of chromosomal aberrations induced by oxidative and genotoxic stress. Leukemia. 2008;22:1969-72.
12. Koptyra M, Falinski R, Nowicki MO, et al. BCR/ABL kinase induces self-mutagenesis via reactive oxygen species to encode imatinib resistance. Blood. 2006;108:319-27.
13. Skorski T. Chronic myeloid leukemia cells refractory/resistant to tyrosine kinase inhibitors are genetically unstable and may cause relapse and malignant progression to the terminal disease state. Leuk Lymphoma 2011;52 Suppl 1:23-9.
14. Petzer AL, Eaves CJ, Barnett MJ, Eaves AC. Selective expansion of primitive normal hematopoietic cells in cytokine-supplemented cultures of purified cells from patients with chronic myeloid leukemia. Blood. 1997;90:64-9.
15. Pihlajamaki J, Boes T, Kim EY, et al. Thyroid hormone-related regulation of gene expression in human fatty liver. J Clin Endocrinol Metab 2009;94:3521-9.
16. Xu F, Ackerley C, Maj MC, et al. Disruption of a mitochondrial RNA-binding protein gene results in decreased cytochrome b expression and a marked reduction in ubiquinol-cytochrome c reductase activity in mouse heart mitochondria. Biochem J 2008;416:15-26.
17. Jung HJ, Shim JS, Lee J, et al. Terpestacin inhibits tumor angiogenesis by targeting UQCRB of mitochondrial complex III and suppressing hypoxia-induced reactive oxygen species production and cellular oxygen sensing. J Biol Chem 2010;285:11584-95.
18. Hitosugi T, Fan J, Chung TW, et al. Tyrosine phosphorylation of mitochondrial pyruvate dehydrogenase kinase 1 is important for cancer metabolism. Mol Cell 2011;44:864-77.

Figure legends:

Figure 1. Expression of OXPHOS genes is altered in CML. (**A**) Differential expression (GO ANOVA) of genes involved in OXPHOS in stem and progenitor populations in CML and normal hematopoiesis; n = number of donors. (**B**) Heat map (One way ANOVA) identifying individual genes involved in OXPHOS which are significantly upregulated (red) or downregulated (blue) when compared to normal HSCs (gray). Results from HSCs and LSCs are highlighted in yellow boxes.

Figure 2. Expression of genes identified by the IFT "Oxidative Phosphorylation" is altered in CML. Heat map (One way ANOVA) identifying individual genes, which are significantly upregulated (red) or downregulated (blue) when compared to normal HSCs (gray). Results from HSCs and LSCs are highlighted in yellow boxes.

Figure 3. Expression of genes identified by the IFT "Mitochondrial Dysfunction" is altered in CML. Heat map (One way ANOVA) identifying individual genes, which are significantly upregulated (red) or downregulated (blue) when compared to normal HSCs (gray). Results from HSCs and LSCs are highlighted in yellow boxes.

Figure 4. Expression of genes encoding the components of MRC is altered in CML-CP LSCs and is not affected by imatinib. (**A**) Modified IPA of the expression of genes encoding MRC in CML-CP LSCs in comparison to normal HSCs. (**B**) Modified IPA of the expression of

genes encoding MRC in the untreated versus imatinib-treated LSCs from CML-CP. Upregulated and downregulated genes are marked in red and blue, respectively.

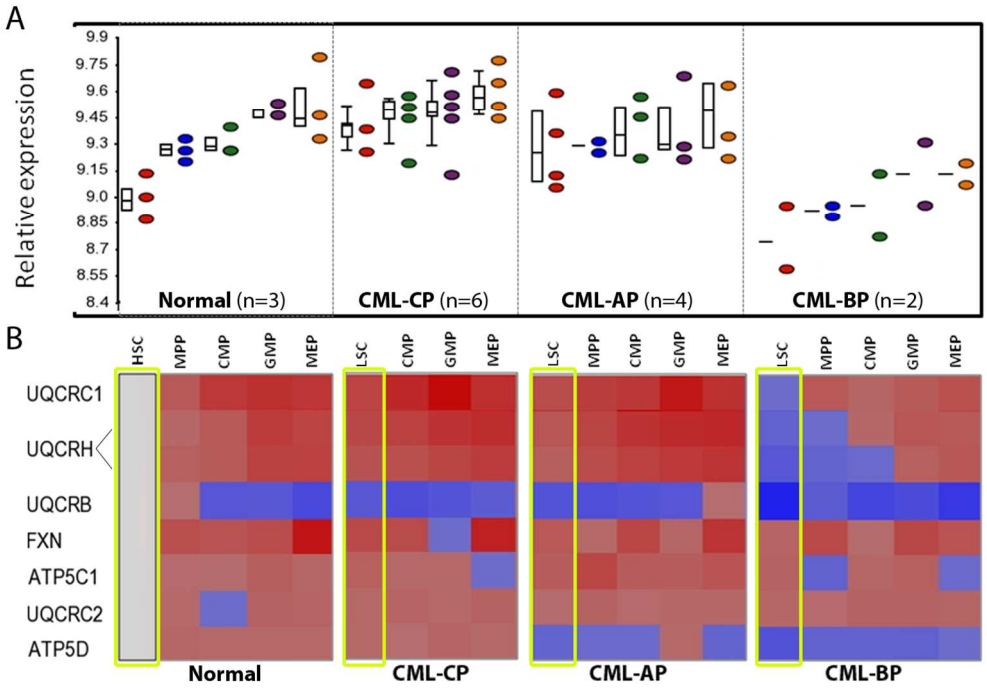
A
Relative expression
9.9
9.75
9.6
9.45
9.3
9.15
9.0
8.85
8.7
8.55
8.4
Normal (n=3)
CML-CP (n=6)
CML-AP (n=4)
CML-BP (n=2)
B
HSC
MPP
CMP
GMP
MEP
LSC
UQCRC1
UQCRH
UQCRB
FXN
ATP5C1
UQCRC2
ATP5D
Normal
CML-CP
CML-AP
CML-BP

Figure 1

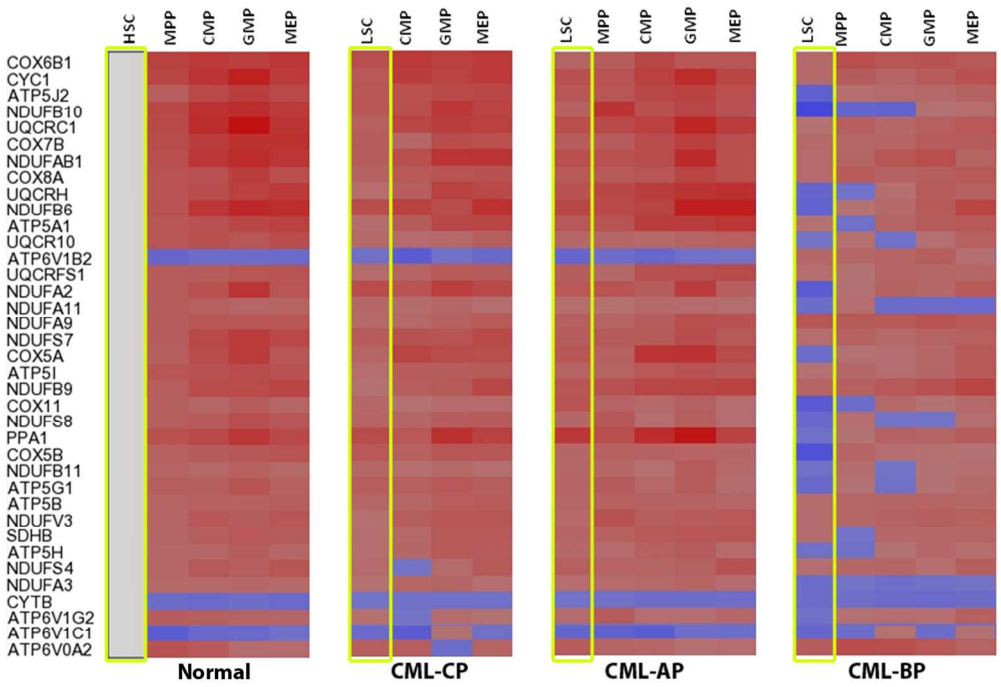
HSC
MPP
CMP
GMP
MEP
LSC
CMP
GMP
MEP
LSC
MPP
CMP
GMP
MEP
LSC
MPP
CMP
GMP
MEP
COX6B1
CYC1
ATP5J2
NDUFB10
UQCRC1
COX7B
NDUFAB1
COX8A
UQCRH
NDUFB6
ATP5A1
UQCR10
ATP6V1B2
UQCRFS1
NDUFA2
NDUFA11
NDUFA9
NDUFS7
COX5A
ATP5I
NDUFB9
COX11
NDUFS8
PPA1
COX5B
NDUFB11
ATP5G1
ATP5B
NDUFV3
SDHB
ATP5H
NDUFS4
NDUFA3
CYTB
ATP6V1G2
ATP6V1C1
ATP6V0A2
Normal
CML-CP
CML-AP
CML-BP

Figure 2

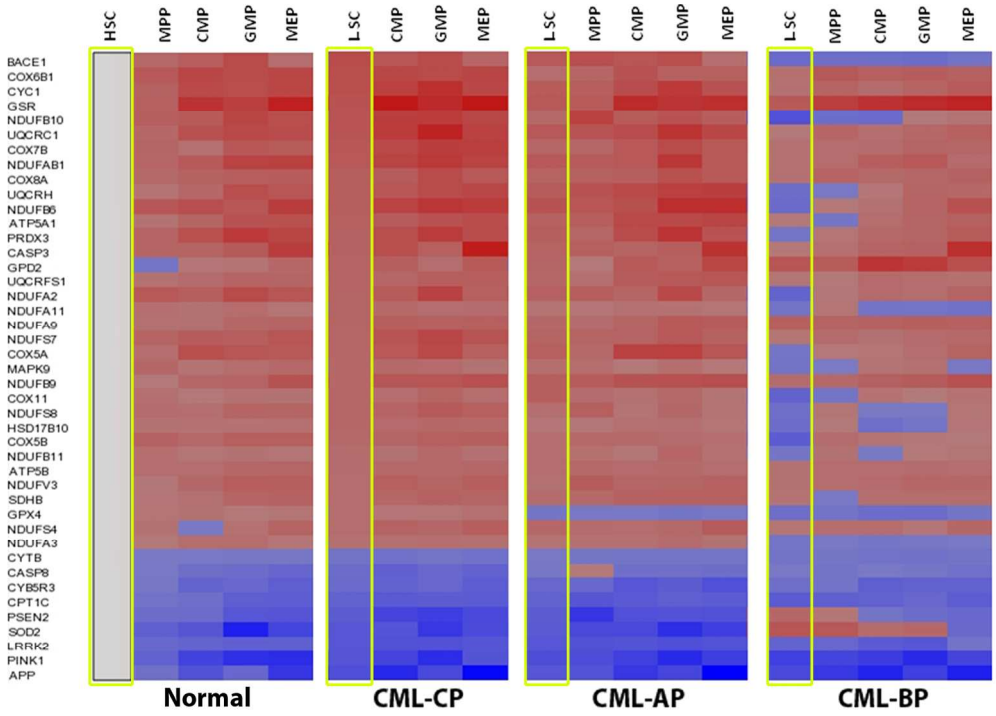
HSC
MPP
CMP
GMP
MEP
LSC
CMP
GMP
MEP
LSC
MPP
CMP
GMP
MEP
LSC
MPP
CMP
GMP
MEP
BACE1
COX6B1
CYC1
GSR
NDUFB10
UQCRC1
COX7B
NDUFAB1
COX8A
UQCRH
NDUFB6
ATP5A1
PRDX3
CASP3
GPD2
UQCRFS1
NDUFA2
NDUFA11
NDUFA9
NDUFS7
COX5A
MAPK9
NDUFB9
COX11
NDUFS8
HSD17B10
COX5B
NDUFB11
ATP5B
NDUFV3
SDHB
GPX4
NDUFS4
NDUFA3
CYTB
CASP8
CYB5R3
CPT1C
PSEN2
SOD2
LRRK2
PINK1
APP
Normal
CML-CP
CML-AP
CML-BP

Figure 3

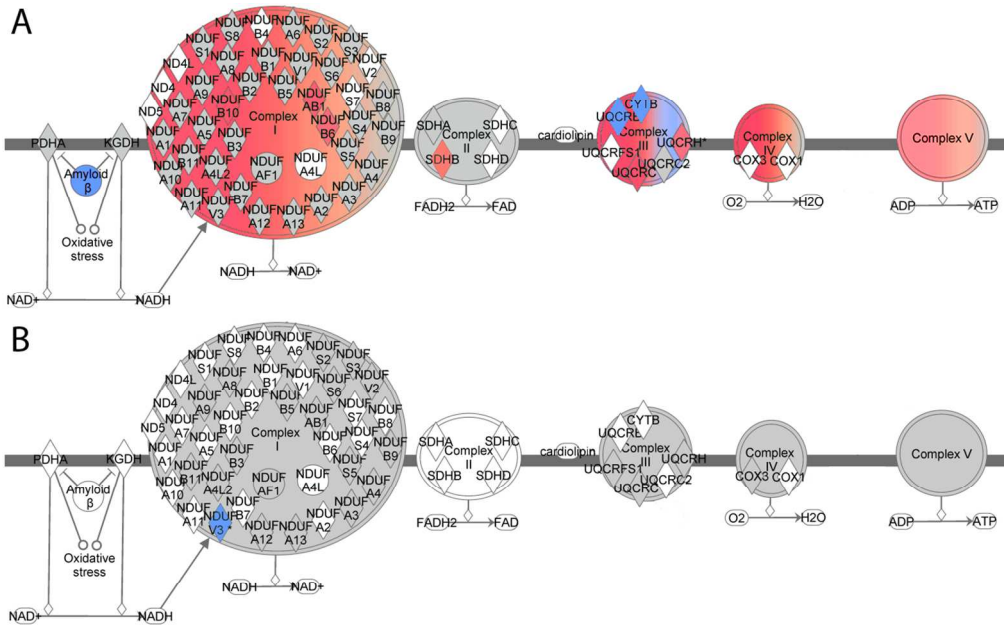
A
PDHA
KGDH
Amyloid β
Oxidative stress
NAD+
NADH
Complex I
NADH
NAD+
SDHA
SDHB
Complex II
SDHC
SDHD
FADH2
FAD
cardiolipin
CYTB
UQCRL
Complex III
UQCRFS1
UQCRH
UQCRC2
Complex IV
COX3
COX1
O2
H2O
Complex V
ADP
ATP
B
PDHA
KGDH
Amyloid β
Oxidative stress
NAD+
NADH
Complex I
NADH
NAD+
SDHA
SDHB
Complex II
SDHC
SDHD
FADH2
FAD
cardiolipin
CYTB
UQCRL
Complex III
UQCRFS1
UQCRH
UQCRC2
Complex IV
COX3
COX1
O2
H2O
Complex V
ADP
ATP

Figure 4

Supplemental Table 1. **Oxidative phosphorylation (GO-ID: 6119): CML-CP LSCs versus normal HSCs**

Gene	P value	Fold change
UQCRC1	0.000654	1.68953
UQCRH	0.006115	1.60273
FXN	0.127043	1.58157
UQCRH	0.015351	1.44236
ATP5C1	0.251449	1.21661
UQCRC2	0.425902	1.08918
ATP5D	0.608306	1.06473
UQCRB	0.039072	-1.35077

Supplemental Table 2. **: Ingenuity Functional Term – "Oxidative phosphorylation" CML-CP LSCs versus normal HSCs**

Gene	P value	Fold change	Gene	P value	Fold change
COX6B1	2.51E-06	1.87427	**ATP5I**	0.000165	1.51763
CYC1	3.36E-05	1.82446	**NDUFB9**	0.001193	1.37055
ATP5J2	0.007985	1.38781	**COX11**	0.050168	1.36562
NDUFB10	0.015792	1.76151	**NDUFS8**	0.044569	1.36554
UQCRC1	0.000136	1.75859	**PPA1**	0.014709	1.60698
COX7B	0.000308	1.69678	**COX5B**	0.094807	1.33068
NDUFAB1	0.003011	1.6692	**NDUFB11**	0.007921	1.28617
COX8A	0.000102	1.56086	**ATP5G1**	0.005954	1.38345
UQCRH	0.007048	1.55962	**ATP5B**	0.00081	1.27892
NDUFB6	0.011922	1.55013	**NDUFV3**	0.01493	1.26489
ATP5A1	0.00226	1.50946	**SDHB**	0.014166	1.25953
UQCR10	0.000227	1.51849	**ATP5H**	0.043746	1.2302
ATP6V1B2	0.025858	-1.23528	**NDUFS4**	0.091942	1.24174
UQCRFS1	0.006097	1.43215	**NDUFA3**	0.054158	1.19568
NDUFA2	0.013035	1.41154	**CYTB**	0.012989	-1.12641
NDUFA11	0.020686	1.40854	**ATP6V1G2**	0.002426	1.39659
NDUFA9	0.000335	1.40673	**ATP6V1C1**	0.005832	-1.39083
NDUFS7	0.01449	1.39788	**ATP6V0A2**	0.005499	1.58971
COX5A	0.070689	1.38152			

Supplemental Table 3. **: Ingenuity Functional Term "Mitochondrial Dysfunction" CML-CP LSCs versus normal HSCs**

Gene	P value	Fold change	Gene	P value	Fold change
BACE1	0.000289	1.88839	**NDUFB9**	0.001193	1.37055
COX6B1	2.51E-06	1.87427	**COX11**	0.050168	1.36562
CYC1	3.36E-05	1.82446	**NDUFS8**	0.044569	1.36554
GSR	2.28E-05	1.76463	**HSD17B10**	0.005019	1.35441
NDUFB10	0.015792	1.76151	**COX5B**	0.094807	1.33068
UQCRC1	0.000136	1.75859	**NDUFB11**	0.007921	1.28617
COX7B	0.000308	1.69678	**ATP5B**	0.00081	1.27892
NDUFAB1	0.003011	1.6692	**NDUFV3**	0.01493	1.26489
COX8A	0.000102	1.56086	**SDHB**	0.014166	1.25953
UQCRH	0.007048	1.55962	**GPX4**	0.049485	1.248
NDUFB6	0.011922	1.55013	**NDUFS4**	0.091942	1.24174
ATP5A1	0.00226	1.50946	**NDUFA3**	0.054158	1.19568
PRDX3	0.002291	1.46893	**CYTB**	0.012989	-1.12641
CASP3	0.025413	1.4658	**CASP8**	0.036249	-1.27424
GPD2	0.027559	1.44514	**CYB5R3**	0.005975	-1.28788
UQCRFS1	0.006097	1.43215	**CPT1C**	2.61E-05	-1.4606
NDUFA2	0.013035	1.41154	**PSEN2**	0.024165	-1.57809
NDUFA11	0.020686	1.40854	**SOD2**	0.053969	-1.68882
NDUFA9	0.000335	1.40673	**LRRK2**	1.48E-07	-1.70011
NDUFS7	0.01449	1.39788	**PINK1**	0.000158	-1.74063
COX5A	0.070689	1.38152	**APP**	3.03E-06	-1.85859
MAPK9	0.00297	1.37965			

Supplemental Table 4.: **MRC complex I-V gene expression levels in the untreated versus imatinib-treated CML-CP LSCs.**

Probeset ID	Gene	P value	Fold change		Probeset ID	Gene	P value	Fold change
1. Mitochondrial complex I: NADH dehydrogenase (ubiquinone) subunits								
202298_at	**NDUFA1**	0.867183	1.10158		203613_s_at	**NDUFB6**	0.466514	1.33051
222971_at	**NDUFA2**	0.905607	1.01233		1559042_at	**NDUFB6**	0.277021	-1.04994
209223_at	**NDUFA2**	0.158368	-1.30049		202839_s_at	**NDUFB7**	0.148330	1.12865
209224_s_at	**NDUFA2**	0.937902	-1.02965		211407_at	**NDUFB7**	0.486221	-1.12377
218563_at	**NDUFA3**	0.859866	-1.09639		201227_s_at	**NDUFB8**	0.727341	1.23805
217773_s_at	**NDUFA4**	0.819815	1.15072		214241_at	**NDUFB8**	0.739387	-1.03214
218484_at	**NDUFA4L2**	0.290043	1.11992		201226_at	**NDUFB8**	0.755049	1.12722
215850_s_at	**NDUFA5**	0.477794	1.04157		222992_s_at	**NDUFB9**	0.821917	1.11209
201304_at	**NDUFA5**	0.827338	-1.15452		223112_s_at	**NDUFB10**	0.305749	-1.15135
202001_s_at	**NDUFA6**	0.672114	1.50434		228301_x_at	**NDUFB10**	0.714177	-1.07149
202000_at	**NDUFA6**	0.397883	-1.31214		218320_s_at	**NDUFB11**	0.775565	1.05712
1557532_at	**NDUFA7**	0.713307	1.06157		203478_at	**NDUFC1**	0.919001	1.06758
202785_at	**NDUFA7**	0.665959	-1.04726		232146_at	**NDUFC1**	0.760959	-1.01626
218160_at	**NDUFA8**	0.565271	1.33916		218101_s_at	**NDUFC2**	0.941795	1.05062
208969_at	**NDUFA9**	0.850008	-1.05655		222521_x_at	**NDUFC2**	0.855177	-1.01445
227206_at	**NDUFA10**	0.128318	-1.08268		229647_at	**NDUFS1**	0.560758	1.13935
1555548_at	**NDUFA10**	0.485857	-1.12956		236356_at	**NDUFS1**	0.979558	1.00207
1554719_at	**NDUFA10**	0.612086	-1.05685		239268_at	**NDUFS1**	0.156351	-1.03485
217860_at	**NDUFA10**	0.727667	-1.11972		235321_at	**NDUFS1**	0.682528	-1.03471
225304_s_at	**NDUFA11**	0.570616	1.07569		203039_s_at	**NDUFS1**	0.781332	-1.12214
228689_at	**NDUFA11**	0.546424	-1.06260		201966_at	**NDUFS2**	0.356585	1.30053
228690_s_at	**NDUFA11**	0.845222	-1.12040		201740_at	**NDUFS3**	0.687337	-1.24745
223244_s_at	**NDUFA12**	0.772277	1.30788		209303_at	**NDUFS4**	0.512921	1.14782
220864_s_at	**NDUFA13**	0.902751	-1.05405		1555057_at	**NDUFS4**	0.281542	-1.03651
202077_at	**NDUFAB1**	0.773993	1.15994		201757_at	**NDUFS5**	0.769222	1.25458
243630_at	**NDUFB1**	0.549958	1.04223		203606_at	**NDUFS6**	0.896025	1.11308
206790_s_at	**NDUFB1**	0.611159	1.24158		242168_at	**NDUFS7**	0.500249	1.05153
218200_s_at	**NDUFB2**	0.763360	1.20478		211752_s_at	**NDUFS7**	0.079138	-1.09532
240391_at	**NDUFB2**	0.196730	-1.08277		232169_x_at	**NDUFS8**	0.900162	1.07497
218201_at	**NDUFB2**	0.481261	-1.06821		203190_at	**NDUFS8**	0.364762	-1.24645
203371_s_at	**NDUFB3**	0.506174	-1.20467		203189_s_at	**NDUFS8**	0.703119	-1.03706
218226_s_at	**NDUFB4**	0.466680	1.64043		227795_at	**NDUFV1**	0.609766	-1.12617
228940_at	**NDUFB4**	0.901174	1.01031		208714_at	**NDUFV1**	0.782795	-1.11417
203621_at	**NDUFB5**	0.574450	1.25982		202941_at	**NDUFV2**	0.736427	-1.26819
					226616_s_at	**NDUFV3**	**0.021986**	**-1.13033**
2. Mitochondrial complex II: succinate dehydrogenase subunits								
201093_x_at	**SDHA**	0.459680	-1.27657		216591_s_at	**SDHC**	0.642960	1.04136
202675_at	**SDHB**	0.883282	1.03174		215088_s_at	**SDHC**	0.945676	1.03904
214166_at	**SDHB**	0.991117	1.00093		238056_at	**SDHC**	0.957705	-1.00536
202004_x_at	**SDHC**	0.203899	1.40669		215652_at	**SDHD**	0.908240	1.00738
210131_x_at	**SDHC**	0.408984	1.12324		202026_at	**SDHD**	0.975438	-1.00531

Probeset ID	Gene	P value	Fold change		Probeset ID	Gene	P value	Fold change
3. Mitochondrial complex III: ubiquinol-cytochrome c reductase complex subunits								
201066_at	**CYC1**	0.587744	-1.33051		201903_at	**UQCRC1**	0.607226	-1.36365
218190_s_at	**UQCR10**	0.964667	1.01081		212600_s_at	**UQCRC2**	0.848710	1.13128
228142_at	**UQCR10**	0.898268	-1.01408		241755_at	**UQCRC2**	0.203810	-1.06954
202090_s_at	**UQCR11**	0.601351	1.56712		200883_at	**UQCRC2**	0.775845	-1.26770
223613_at	**UQCR11**	0.882728	-1.02446		208909_at	**UQCRFS1**	0.639032	-1.48297
205849_s_at	**UQCRB**	0.518622	1.64366		202233_s_at	**UQCRH**	0.955300	1.03505
209066_x_at	**UQCRB**	0.542853	1.47041		201568_at	**UQCRQ**	0.537262	-1.38722
209065_at	**UQCRB**	0.985410	1.00445					
244293_at	**UQCRB**	0.883126	-1.00542					
4. Mitochondrial complex IV: cytochrome c oxidase subunits								
200086_s_at	**COX4I1**	0.400657	1.50342		201441_at	**COX6B1**	0.648072	1.23983
202698_x_at	**COX4I1**	0.509855	1.64109		1553367_a_at	**COX6B2**	0.903653	-1.02754
213758_at	**COX4I1**	0.244363	-1.16866		201754_at	**COX6C**	0.806479	-1.22889
232761_at	**COX4I2**	0.674413	-1.05780		204570_at	**COX7A1**	0.324356	1.11373
203663_s_at	**COX5A**	0.533099	1.67431		201597_at	**COX7A2**	0.963172	-1.03472
229426_at	**COX5A**	0.896803	1.01955		201256_at	**COX7A2L**	0.688165	1.20520
211025_x_at	**COX5B**	0.800752	1.06496		239252_at	**COX7B**	0.356746	-1.29211
202343_x_at	**COX5B**	0.999996	1.00000		202110_at	**COX7B**	0.787721	-1.26278
213736_at	**COX5B**	0.135785	-1.17547		231265_at	**COX7B2**	0.569338	-1.07830
213735_s_at	**COX5B**	0.994309	-1.00242		213846_at	**COX7C**	0.519717	-1.28219
224344_at	**COX6A1**	0.372780	1.05732		217491_x_at	**COX7C**	0.829521	-1.21148
200925_at	**COX6A1**	0.643732	1.23988		201134_x_at	**COX7C**	0.946748	-1.05321
234876_at	**COX6A1**	0.358854	-1.14119		201119_s_at	**COX8A**	0.821015	-1.07365
206353_at	**COX6A2**	0.382106	-1.16231		231487_at	**COX8C**	0.267065	-1.04426
5. Mitochondrial complex V: ATP synthase subunits								
213738_s_at	**ATP5A1**	0.714095	1.34846		210149_s_at	**ATP5H**	0.500637	-1.28354
1569891_at	**ATP5A1**	0.955786	-1.00854		1555998_at	**ATP5H**	0.835896	-1.03300
201322_at	**ATP5B**	0.746834	-1.34473		209492_x_at	**ATP5I**	0.805656	1.18158
205711_x_at	**ATP5C1**	0.792557	1.27375		207335_x_at	**ATP5I**	0.864985	1.08965
213366_x_at	**ATP5C1**	0.827924	1.20394		202325_s_at	**ATP5J**	0.962204	-1.04835
208870_x_at	**ATP5C1**	0.960874	1.04372		202961_s_at	**ATP5J2**	0.958668	1.05726
214132_at	**ATP5C1**	0.568208	-1.06196		1558179_at	**ATP5J2**	0.500469	-1.06377
203926_x_at	**ATP5D**	0.144014	-1.18691		208745_at	**ATP5L**	0.112297	2.25655
213041_s_at	**ATP5D**	0.315207	-1.30603		208746_x_at	**ATP5L**	0.570229	1.52479
217801_at	**ATP5E**	0.919716	1.09008		210453_x_at	**ATP5L**	0.732132	1.29884
230535_s_at	**ATP5E**	0.388714	-1.03942		207573_x_at	**ATP5L**	0.751791	1.20839
211755_s_at	**ATP5F1**	0.668729	1.70501		200818_at	**ATP5O**	0.658107	1.56786
243501_at	**ATP5F1**	0.681419	1.00573		216954_x_at	**ATP5O**	0.877471	1.07834
208972_s_at	**ATP5G1**	0.690204	-1.24543		1564482_at	**ATP5O**	0.255337	-1.10591
208764_s_at	**ATP5G2**	0.838677	1.07683		223338_s_at	**ATPIF1**	0.370273	1.32505
207552_at	**ATP5G2**	0.985030	1.00196		218671_s_at	**ATPIF1**	0.750222	1.18601
207507_s_at	**ATP5G3**	0.761873	1.19014		223339_at	**ATPIF1**	0.164763	-1.18296
207508_at	**ATP5G3**	0.825819	1.24125					
228168_at	**ATP5G3**	0.899934	-1.00806					